© SEP 2026 | IRE Journals | Volume 10 Issue 3 | ISSN: 2456-8880
DOI: https://doi.org/10.64388/IREV10I3-1722687

Influence of Water Content on Morphology and Capacitive Performance of TiO_2 Nanotube as Binder Free Supercapacitor Electrode Material Synthesized from Glycerol-Based Electrolyte

MUHAMMAD MUHAMMAD MUZAKIR[1], BUHARI MAGAJI[2], ALIYU AMINU SISA[3]
[1, 2]*Department of Chemical Sciences, Faculty of Science, Gombe State University, Gombe, Nigeria.*
[3] *Department of Pure and Applied Physics, Faculty of Science, Gombe State University, Gombe, Nigeria.*

Abstract- ***Highly ordered titania nanotubes (TNTs) as a 1D nanostructured material have received a lot of interest for supercapacitor applications due to their large surface area and relatively low cost. The structural and capacitive optimization of anodic TiO_2 nanotube arrays via electrolyte hydration over broad concentration ranges remains underexplored. This study systematically investigates the effect of water content (5 to 90 vol%) in a glycerol/NH_4F electrolyte on the morphology and charge-storage performance of TiO_2 synthesized at a constant potential of 20 V for 60 minutes. Morphological analysis reveals a strict hydration dependency for tubular growth; from ultra-low (5 vol%) and ultra-high (90 vol%) water concentrations which fail to produce nanotubes, yielding instead cracked surfaces with etching pits and non-porous passive films, respectively. Within the favorable formation window, increasing the water content from 25 to 70 vol% drives a continuous decrease in average tube diameter, from 62 nm to 43 nm at 25 and 70 vol%, respectively due to accelerated field-assisted chemical dissolution at lower electrolyte viscosities. Electrochemical characterization demonstrates that this morphological evolution directly dictates charge-storage capabilities. A maximum areal capacitance of 240 µF/cm² was achieved at 50 vol% water, significantly outperforming the 25 vol% (180 µF/cm²) and 70 vol% (150 µF/cm²) architectures due to an optimized balance of electrochemically active surface area and structural integrity. Conversely, the non-tubular architectures at 5 vol% and 90 vol% exhibit exceptionally poor capacitances of 30 and 20 µF/cm². These findings highlight the critical role of tuning electrolyte viscosity and dissolution kinetics to maximize the capacitive performance of titanium-based energy storage devices.***

Keywords: water content, tio₂ nanotubes, supercapacitor, glycerol electrolyte, morphology, areal capacitance.

I. INTRODUCTION

Development and design of clean, renewable, and sustainable energy storage devices have increased in recent years due to increasing energy consumption, rapid depletion of fossil fuels and worsening environmental pollution [1]. Thus, finding new, highly efficient, low cost and environmentally friendly energy storage systems is undoubtedly important considering the needs of modern technology developments in the world today [2]. In this context, supercapacitors (SCs) also known as electrochemical capacitors (ECs) or ultracapacitors have gained great attention from researchers worldwide owing to their ability to bridge the performance gap between batteries and conventional capacitors in terms of high energy and power densities and long-term cycling stability [3]. These advantages of SCs make them suitable for many potential applications in different industrial technology as energy storage devices.

One-dimensional (1D) nanostructure materials such as tubes, wires, rods, belts have found widespread applications because of their exceptional properties in terms of high surface area and electrical conductivity offering rapid electron transport and chemical reactivity. In addition, they can serve as interconnectors for fabrication of electrochemical devices such as SCs with nanoscale dimension [4]. Titanium dioxide (TiO_2) or titania has been used as active electrode material in supercapacitor applications [5-6] due to its unique properties such as high chemical stability, non-toxicity, low cost, developed surface area and biocompatibility [7-8]. However, compact titania exhibits low specific surface area and only contribute very low areal

capacitance of 10-40 μF/cm^2 due to the high electrical resistance which prevents fast electron transfer [9]. Although nanocrystalline titania can increase the specific surface area of the supercapacitor electrode, the addition of binder which is an important step in electrode preparation can reduce the interconnectivity of the active titania nanoparticles with the current collector. This results in increase in resistance of the electrode apart from the additional cost.

To overcome the problem associated with compact and nanocrystalline titania, titania nanotubes (TNTs) obtained by electrochemical anodization was used due to its high accessible surface area and unique pathways resulted from the hollow structures for electron transport and short diffusion pathways for electrolytes. This fabrication route provides highly ordered; well separated nanotubes directly grown on the current collector (Ti foil) which can be used as a binder-free electrode.

Electrochemical anodization of titanium foils in viscous organic electrolytes, predominantly glycerol or ethylene glycol containing fluoride salts such as ammonium fluoride (NH_4F) has emerged as a premier pathway for synthesizing vertically aligned TiO_2 nanotube arrays (TNTAs). Previous studies establish that water addition triggers fundamental morphological shifts in organic anodization baths, in ultra-low water (< 2 – 5 vol%) or near-anhydrous organic media, high solution viscosity restricts ionic transport [10-11]. This limited ion mobility restricts localized chemical dissolution, frequently leading to thick barrier layers, low aspect ratios, or non-uniform tubular growth, while introducing controlled quantities of water in the range of 5 – 15 vol% lowers kinematic viscosity and enhances ionic conductivity without compromising structural integrity [12-14]. This balance stabilizes the oxidation-dissolution front, yielding high-aspect-ratio, smooth-walled, vertically aligned nanotube arrays with enlarged inner diameters and optimal tube lengths. On the other hand, high water content (> 25 vol%) beyond critical hydration thresholds, the dramatic drop in viscosity accelerates chemical dissolution at the tube mouth. Localized chemical etching by H^+ and F^- outpaces steady-state oxidation at the substrate interface. This imbalance causes top-wall thinning, leading to "nanograss" collapse (tangled, fallen nanotube tips), shortened tube lengths, or a complete transition into unorganized porous oxide films [15-17].

Despite extensive literature on anodic TiO_2 nanostructures, two key limitations persist; most existing investigations restrict water parameter screening to narrow, low-concentration ranges (0 – 10 vol%, at most 50 vol%) aimed solely at geometric optimization, neglecting broader concentration behavior. Investigations isolating water content across a broad range under strictly fixed potential and fixed time constraints remain underreported. This work addresses these gaps by systematically evaluating the 5 – 90 vol% water ratio spectrums in a glycerol/NH_4F electrolyte under fixed anodization conditions (20 V, 60 minutes). By decoupling water content from potential and time variations, this study establishes the quantitative relationships connecting electrolyte hydration, morphological stability thresholds, and resulting electrochemical charge-storage capabilities.

II. MATERIALS AND METHODS

2.1 Synthesis of Titania Nanotubes

The purchased titanium foil (0.25 mm thickness, 99.7% purity, Sigma-Aldrich) was cut into small pieces of 1 × 1 cm with extra 1 cm used as holder of the electrode as shown in Figure 1. Prior to anodization, the cut foils were degreased by subsequent sonication in acetone, isopropanol (MERCK) and deionized (DI) water (Millipore Corp., resistivity 18.2 MΩ cm at 25 °C) each for 15 min. The foils were then etched in 6 M HNO_3 acid (65%, MERCK) for 10 min. Finally, the foils were rinsed thoroughly with excess DI water, and dried in air.

© SEP 2026 | IRE Journals | Volume 10 Issue 3 | ISSN: 2456-8880
DOI: https://doi.org/10.64388/IREV10I3-1722687

Figure 1. Ti foil cut into desired dimensions of 1×1 cm (1 cm extra was used as electrode holder)

Titania nanotubes (TNTs) synthesis by electrochemical anodization was carried out as previously reported [18] in a two-electrode cell configuration by employing the Ti foil as the anode and a high-density graphite as the cathode. The two electrodes were kept at 3 cm distance in all experiments. The anodization electrolyte consists of 0.5 wt% NH_4F dissolved in a mixture of glycerol (G) (99.8% purity, initial water content 0.03 wt%, Fisher Scientific) and different volume of DI water (v/v%). The anodization was conducted at fixed anodization voltage of 20 V for 60 minutes. All experiments were carried out at room temperature under a constant magnetic stirring (300 rpm) to ensure uniform distribution of electroactive species and temperature in the electrolyte. The anodization voltage was supplied by a DC power supply (Consort Mini, Cleaver Scientific Ltd). After the anodization, the samples were rinsed with DI water, dried in air, and then annealed in open air in furnace at 500 °C for 2 h at a heating rate of 2 °C/min.

2.2 Influence of Water Content

To study the influence of water content on the morphology and capacitive performance of the TNTs, the anodization was conducted at different volumes of DI water containing 0.5 wt% NH_4F as described which will be referred to as $NH_4F/G/H_2O$ henceforth. The water content in $NH_4F/G/H_2O$ was varied to 5, 25, 50, 70, and 90 v/v% while fixed volume of glycerol was used accordingly. The anodization was conducted at 20 V for 1 h.

2.3 Characterization of the Synthesized Samples

The optimized sample in this study (TNTs 50%) was characterized using different equipment such as X-ray diffraction (XRD), while all the samples synthesized at different water content were characterized by field emission scanning electron microscopy (FESEM). The electrochemical analysis was conducted using a potentiostat/galvanostat of Autolab PGSTAT204 model equipped with FRA32M module.

III. RESULTS AND DISCUSSION

3.1 X-ray Diffraction

The XRD pattern of optimized TNTs at 50 vol% before and after calcination at 500 °C for 2 h are presented in Figure 2. Before calcination, only peaks corresponding to the titanium (Ti) substrate were observed at $2\boldsymbol{\theta}$= 35.1°, 38.4°, 40.2°, 53.2°, 63.0°, 71.0°, and 77.4°, indexed to hexagonal Ti (JCPDS: 00-044-1294). This indicates that the as-anodized TNTs are amorphous in nature and thus only diffraction peaks for Ti substrate were observed. This result is consistent with other findings [19-20]. Upon calcination, new peaks appeared at $2\boldsymbol{\theta}$= 25.7° and 48.5° which are both indexed to (101) and (200) planes of anatase phase respectively (JCPDS: 01-075-1537). This shows that at 500 °C calcination temperature, the preferred growth orientation of the TNTs is anatase phase as the rutile phase usually starts to appear at higher temperature from 550 °C and a complete transformation to rutile is usually achieved from temperature above 700 °C [21].

3.2 Field Emission Scanning Electron Microscopy

Generally, the self-organizing architecture of TNTs arrays is governed by a dynamic competition between field-assisted oxidation at the metal/oxide interface (Eq. 1) and field-assisted chemical dissolution of the oxide by fluoride complexes at the pore bottom (Eq. 2): (Berger et al., 2010; Al-Waisawy et al., 2022).

$$Ti + 2H_2O \longrightarrow TiO_2 + 4H^+ + 4e^- \quad (1)$$

$$TiO_2 + 6F^- + 4H^+ \longrightarrow [TiF_6]^{2-} + 2H_2O \quad (2)$$

Within this dual-process mechanism, water acts as an active chemical participant and a primary fluidic

© SEP 2026 | IRE Journals | Volume 10 Issue 3 | ISSN: 2456-8880
DOI: https://doi.org/10.64388/IREV10I3-1722687

modulator. As the primary oxygen donor, water sustains oxide film growth. Simultaneously, its volumetric ratio directly tunes electrolyte viscosity, ionic conductivity, and the diffusion kinetics of species such as F^-, OH^-, and $[TiF_6]^{2-}$[14, 16].

Figure 3 displays the surface view of FESEM images synthesized at different water contents. At 5% water content (Figure 3a), the TNTs are showing cracked surface with some tiny etching pits indicates slow oxide formation which results in surface stress and roughness. In highly viscous organic electrolyte such as glycerol (viscosity (η) = 945 cP at 25 °C) [22], the only source of oxygen is generally the added water, as oxygen in glycerol is strongly bonded to carbon, at this low water content, the formation of compact oxide layer on titanium surface is limited and thus a decreased in chemical dissolution leading to formation of only tiny pits instead of nanopores.

Upon addition of water to 25%, the TNTs were transformed to a circular, ordered, separated tubes with well-defined tubes wall (Figure 3b). This indicates fast oxide formation and increase dissolution rate of TiO_2 layer at this water content. Increasing the water content to 50% results in less dense, disordered tubes that tend to crumble with increased tube-tube spacings (Figure 3c).

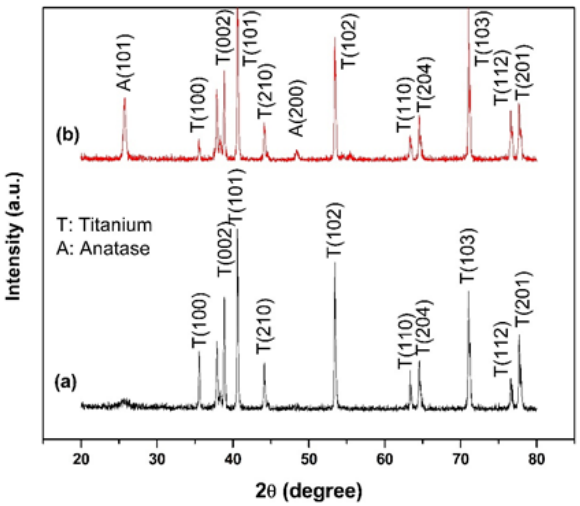

Figure 2. XRD pattern of optimized TNTs obtained at 50% water content, 20 V, for 60 min anodization voltage and time (a) as-anodized TNTs, (b) TNTs calcined at 500 °C.

This might be ascribed to faster chemical dissolution at the bottom of the nanotubes caused by F^- ions under the electric field which may migrate faster through oxide layer to form fluoride-rich layer at metal/oxide interface. However, when water content is increase to 70%, the TNTs eventually crumble and resulted in nanoporous structure (Figure 3d) because of high-rate dissolution of the fluoride-rich layer. at the bottom of tubes by higher water content, in addition to the etching at the top of the tubes [15].

Further increase in water content to 90%, results in non-formation of porous or tubular structure (Figure 3e), in this case the F^- concentration may be low considering the high content of water in the electrolyte, and insufficient to promote the chemical dissolution of the oxide layer [23]. In addition, the electrophoresis power supply used for the anodization shows a sharp drop in current (< 1 mA) that prompt the anodization to stop after proceeding for only 5 min. This indicates poor conductivity of the electrolyte at this higher water content.

From the different morphology of TNTs images presented in Figure 3a-e, we can clearly see how water content in $NH_4F/G/H_2O$ plays key role in determining the structure and morphology of the synthesized TNTs in terms of oxide layer formation and transformation from nanoporous to nanotubular structures [24-25]. Among all the tube morphologies, tube diameter influences the TNTs morphology most significantly in determining the final properties of synthesized TNTs. To this end, water content was found to affect the tube diameter, the average tube diameter at 25, 50, and 70% water content, measured by image analysis software 'Image J' was obtained to be 62, 53, and 43 nm, respectively.

3.3 Electrochemical Properties of Synthesized Titania Nanotubes.

The influence of water content on capacitive performance of synthesized TNTs was investigated by cyclic voltammetry (CV) and galvanostatic charge discharge (GCD) measurements of all the samples. The CV and GCD analysis were carried out over potential range of 0.0 to 1.0 V at different scan rates (20-200 mV s^{-1}) and current densities (10-50 µA cm^{-2}).

CV voltammograms of all the TNTs samples synthesized at 5, 25, 50, 70, and 90 v/v% water content refer to henceforth as TNTs 5%, TNTs 25%, TNTs 50%, TNTs 70%, and TNTs 90% respectively, obtained at scan rate of 20 mV s^{-1} are presented in Figure 4a. All the samples exhibit a distorted symmetrical shape with no redox peaks, indicating electric double layer capacitance (EDLC) behavior. The distorted anodic regions implied low electrochemical activity of TNTs at anodic potential above 0.3 V.

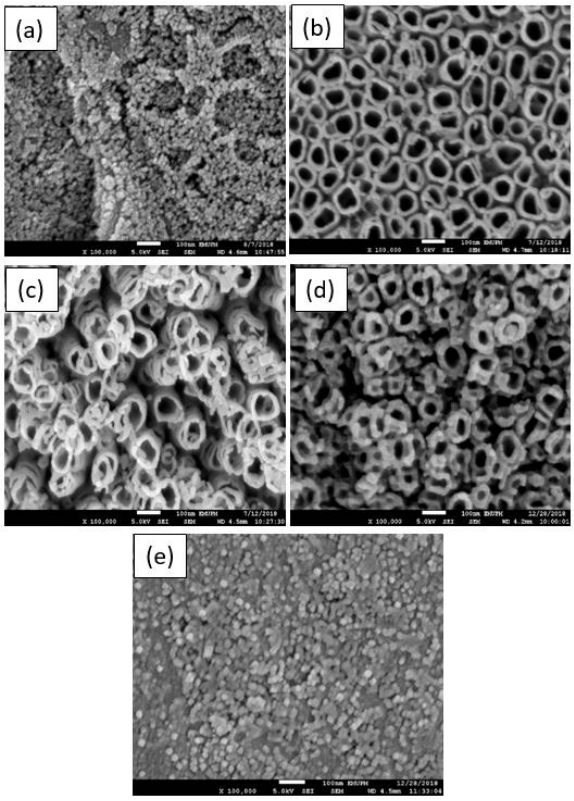

Figure 3. Surface view FESEM images of TNTs synthesized in (a) 5, (b) 25, (c) 50, (d) 70, and (e) 90 v/v% water content at constant voltage of 20 V for 1h.

The sample TNTs 50% shows higher current density and larger integrated area compared to other samples which indicates enhancement in capacitive performance of the sample. Although from FESEM images, TNTs 25% shows more vertically aligned nanotubes with larger tube diameter than TNTs 50%. However, the nanoporous structure and larger tube to tube spacing exhibit by TNTs 50% can provide more surface area leading to higher capacitive performance. It is suggested that a nanotubular structure with well-separated, larger tube to tube spacing offer higher capacitance in charge storage applications such as supercapacitor contrary to photocatalytic applications [6].

The capacitive performance of the samples was confirmed by GCD at current density of 20 μA/cm^2 as shown in Figure 4b. All the samples exhibit a symmetrical triangular charge discharge curve, a typical of EDLC electrode, with TNTs 50% displaying longer discharge time than the other samples, indicating a higher capacitive performance of the sample. This supports the result from the CV measurement. The calculated areal capacitance (C_A) of the samples by GCD is in the range of 20-240 μF cm^{-2} as displayed in Table 1. The C_A increased from 30 μF cm^{-2} to 240 μF cm^{-2} at TNTs 50% which recorded the highest capacitance. At TNTs 90%, C_A decreased dramatically to 20 μF/cm^2.

These results revealed that a nanotubular architecture of well separated and define tubes as possessed by TNTs 25% and TNTs 50% samples provide more surface area, aligned and properly oriented structure which offers improved pathway for electron transfer.

© SEP 2026 | IRE Journals | Volume 10 Issue 3 | ISSN: 2456-8880
DOI: https://doi.org/10.64388/IREV10I3-1722687

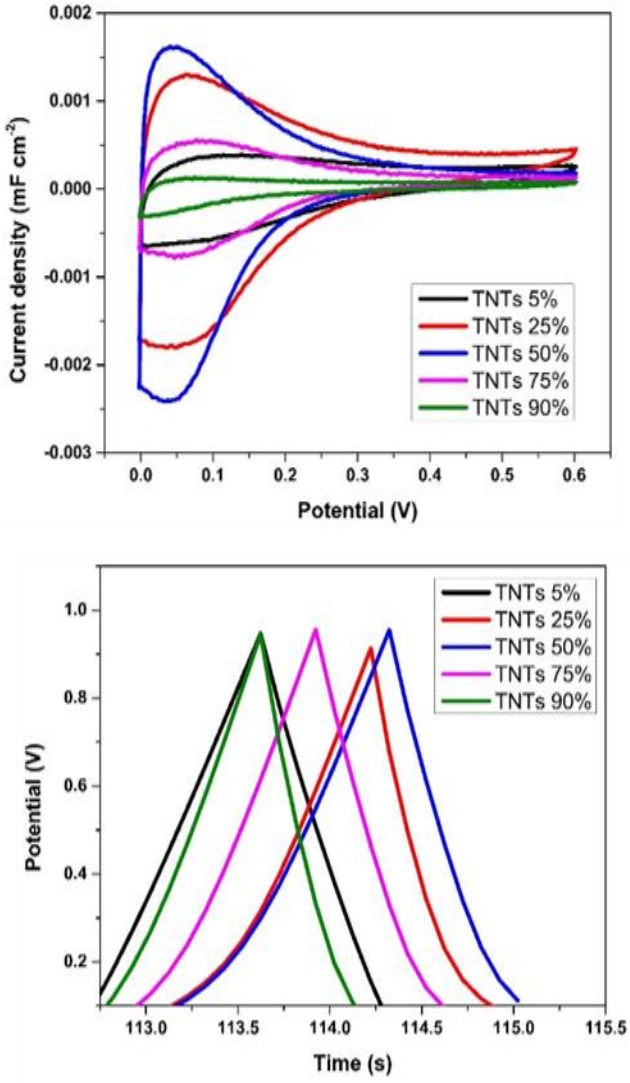

Figure 4. (a) Cyclic voltammograms and (b) GCD curves of TNTs synthesized at 20 V for 1 h at different water contents, collected at scan rate of 20 mV s^{-1} and current density of 20 µA cm^{-2} respectively, in 1 M KCl.

Table 1. Areal capacitance obtained from GCD at current density of 20 µA/cm^2, and average tube diameter of TNTs synthesized at 20 V for 1h at different water contents

Water content (v/v%)	5	25	50	70	90
Average tube diameter (nm)	-	62	53	43	-
Areal capacitance (µFcm^{-2})	30	180	240	150	20

IV. CONCLUSION

This study successfully demonstrates that varying water content across a broad spectrum (5 to 90 vol%) in glycerol/NH_4F electrolytes fundamentally controls both the morphological evolution and the capacitive performance of anodic TiO_2. We identified a defined structural window for successful nanotube formation between 25 and 70 vol% water. Within this regime, tube diameter inversely correlates with hydration, shrinking monotonically from 62 nm to 43 nm as higher water concentrations reduce electrolyte viscosity and accelerate chemical etching kinetics. The transition from nanoporous to nanotubular structure of TiO_2 nanotubes and spacings between the nanotubes was found to depend largely on the water content in the electrolyte, extreme hydration boundaries completely suppress tubular growth, resulting in defective, cracked pitting at 5 vol% and non-porous films at 90 vol%. The structural parameters directly govern electrochemical performance. The highly porous nanotube arrays synthesized at 50 vol% water provide the optimal electrochemically active surface area, delivering a peak areal capacitance of 240 µF/cm². This represents a substantial enhancement over both the wider tubes formed at 25 vol% (180 µF/cm²) and the narrower tubes at 70 vol% (150 µF/cm²), and greatly outperforms the non-tubular extreme conditions (30 µF/cm² and 20 µF/cm²). Ultimately, carefully balancing field-assisted oxidation and chemical dissolution through precise water content modulation is a critical, highly sensitive parameter for optimizing TiO_2 nanotube architectures for energy storage applications.

ACKNOWLEDGMENTS

This research was funded by Tertiary Education Trust Fund (TETFUND) IBR. Authors acknowledge the nomination and all other supports from Gombe State University, Gombe, Nigeria.

REFERENCES

[1] Wu, Z., Li, L., Yan, J. M., & Zhang, X. B. (2017). Materials Design and System Construction for Conventional and New-

Concept Supercapacitors. *Advanced Science*, *4*(6).

[2] Da Silva, L. M., Cesar, R., Moreira, C. M. R., Santos, J. H. M., De Souza, L. G., Pires, B. M., Vicentini, R., Nunes, W., & Zanin, H. (2020). Reviewing the fundamentals of supercapacitors and the difficulties involving the analysis of the electrochemical findings obtained for porous electrode materials. *Energy Storage Materials*, *27*, 555–590.

[3] Afif, A., Rahman, S. M., Tasfiah Azad, A., Zaini, J., Islan, M. A., & Azad, A. K. (2019). Advanced materials and technologies for hybrid supercapacitors for energy storage – A review. *Journal of Energy Storage*, *25*, 100852.

[4] Hou, H., Shao, G., Yang, W., & Wong, W. Y. (2020). One-dimensional mesoporous inorganic nanostructures and their applications in energy, sensor, catalysis and adsorption. *Progress in Materials Science*, *113*, 100671.

[5] Endut, Zulkarnain, Hamdi, M., & Basirun, W. J. (2013b). Optimization and functionalization of anodized titania nanotubes for redox supercapacitor. *Thin Solid Films*, *549*, 306–312.

[6] Salari, M., Aboutalebi, S. H., Chidembo, A. T., Innis, P. C., Konstantinov, K., Liu, H. K., & Schmuki, P. (2014). Design of self-assembled TiO_2 architectures: Towards hybrid nanotubular interfaces. *Physica Status Solidi (A) Applications and Materials Science*, *211*(4), 938–945.

[7] Dvorak, F., Zazpe, R., Krbal, M., Sopha, H., Prikryl, J., Ng, S., Hromadko, L., Bures, F., & Macak, J. M. (2019). One-dimensional anodic TiO2 nanotubes coated by atomic layer deposition: Towards advanced applications. *Applied Materials Today*, *14*, 1–20.

[8] Wawrzyniak, J., Grochowska, K., Karczewski, J., Kupracz, P., Ryl, J., Dołęga, A., & Siuzdak, K. (2020). The geometry of free-standing titania nanotubes as a critical factor controlling their optical and photoelectrochemical performance. *Surface and Coatings Technology*, *389*, 125628.

[9] Salari, M., Aboutalebi, S. H., Konstantinov, K., & Liu, H. K. (2011). A highly ordered titania nanotube array as a supercapacitor electrode. *Physical Chemistry Chemical Physics*, *13*(11), 5038–5041.

[10] Raja, K. S., Gandhi, T., & Misra, M. (2007). Effect of water content of ethylene glycol as electrolyte for synthesis of ordered titania nanotubes. *Electrochemistry Communications*, *9*(5), 1069–1076.

[11] Aiempanakit, C., Junbang, P., Suphap, W., & Aiempanakit, K. (2023). Influence of water content on structural and electrochromic properties of TiO_2 nanotube prepared by anodization. *Journal of Metals, Materials and Minerals*, *33*(3), 1680.

[12] Quiroz, H. P., Quintero, F., Arias, P. J., Dussan, A., & Zea, H. R. (2015). Effect of fluoride and water content on the growth of TiO_2 nanotubes synthesized via ethylene glycol with voltage changes during anodizing process. *Journal of Physics: Conference Series*, *614*(1), 012001.

[13] Naghizadeh, M., Ghannadi, S., Abdizadeh, H., & Golobostanfard, M. R. (2014). Effect of fluoride concentration and water content on morphology of titania nanotubes in ethylene glycol solution. *Advanced Materials Research*, *829*, 907–911.

[14] Al-Waisawy, S., Abdullah, A.K., Hamed, H. A., & Al-bakri, A. A. (2022). Study the effect of water content on the structure of electrochemically prepared TiO_2 nanotubes. *Periodica Polytechnica Electrical Engineering and Computer Science*, *66*(1), 99–104.

[15] Lim, Y. C., Zainal, Z., Hussein, M. Z., & Tan, W. T. (2012). Effect of water content on structural and photoelectrochemical properties of titania nanotube synthesized in fluoride ethylene glycol electrolyte. *Advanced Materials Research*, *501*, 204–208.

[16] Berger, S., Kunze, J., Schmuki, P., Valota, A. T., LeClere, D. J., Skeldon, P., & Thompson, G. E. (2010). Influence of water content on the growth of anodic TiO_2 nanotubes in fluoride-containing ethylene glycol electrolytes. *Journal of The Electrochemical Society*, *157*(1), C18–C23.

[17] Mandić, V., Panžić, I., Kraljić-Roković, M., & Gaboardi, M. (2023). Breakdown of the

anodized nanostructured anatase for photovoltaic devices: The effect of water content in the electrolyte on preparation of large surfaces of nanotubes. *Ceramics International*, *49*(9), 14844–14854.

[18] Muzakir, M. M., Zainal, Z., Abdullah, A. H., Bahrudin, N. H., Lim, H. N., & Mohd Ali, M., S. (2020). Electrochemically Reduced Titania Nanotube Synthesized from Glycerol-Based Electrolyte as Supercapacitor Electrode. *Energies, 13*, 2767.

[19] Lu, X., Wang, G., Zhai, T., Yu, M., & Zhou, L. (2012). Hydrogenated TiO_2 nanotube arrays as high-rate anodes for lithium-ion microbatteries. *Nano Lett.*, *12*, 1690–1696.

[20] Samsudin, N. A., Zainal, Z., Lim, H. N., Sulaiman, Y., Chang, S. K., Lim, Y. C., Ayal, A. K., & Mohd Amin, W. N. (2018). Capacitive performance of vertically aligned reduced titania nanotubes coated with Mn_2O_3 by reverse pulse electrodeposition. *RSC Advances*, *8*(41), 23040–23047.

[21] Salari, M., Aboutalebi, S. H., Chidembo, A. T., Nevirkovets, I. P., Konstantinov, K., & Liu, H. K. (2012). Enhancement of the electrochemical capacitance of TiO_2 nanotube arrays through controlled phase transformation of anatase to rutile. *Physical Chemistry Chemical Physics*, *14*(14), 4770–4779.

[22] Sreekantan, S., Saharudin, K. A., Lockman, Z., & Tzu, T. W. (2010). Fast-rate formation of TiO_2 nanotube arrays in an organic bath and their applications in photocatalysis. *Nanotechnology*, *21*(36).

[23] Rempel, A. A., Valeeva, A. A., Vokhmintsev, A. S., & Weinstein, I. A. (2021). Titanium dioxide nanotubes: synthesis, structure, properties and applications. *Russian Chemical Reviews*, *90*(11), 1397–1414.

[24] Berger, S., Tsuchiya, H., & Schmuki, P. (2008). Transition from Nanopores to Nanotubes : Self-Ordered Anodic Oxide Structures on Titanium-Aluminides. *Chemistry of Materials*, *20*(10), 3245–3247.

[25] Roy, P., Berger, S., & Schmuki, P. (2011b). TiO_2 nanotubes: Synthesis and applications. *Angewandte Chemie - International Edition*, *50*(13), 2904–2939.